Fluorescence Quantification of Extracellular Vesicles Collected from Human Plasma via Dielectrophoresis

Kyle T. Gustafson, Katherine Huynh, Jesus Bueno, Augusta Modestino, Daniel Heineck, Michael Heller, Stuart Ibsen
gustafky@ohsu.edu, huynka@ohsu.edu, Ibsen@ohsu.edu
Cancer Early Detection Advanced Research (CEDAR) Center, Knight Cancer Institute
Department of Biomedical Engineering, Oregon Health & Science University
Portland, OR

DIELECTROPHORESIS

- Dielectrophoresis (**DEP**) is defined as the motion of electrically polarizable objects in the presence of an electric field gradient.[1,2]
- The applied electric field induces an electric dipole moment in an object, which interacts with an electric field gradient.[3]
- Contrast in the dielectric properties an object and its surrounding media is necessary for DEP.

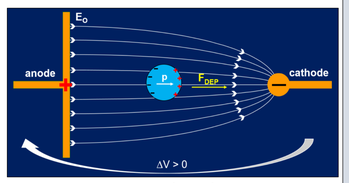

$$F_{DEP} \equiv (\boldsymbol{p} \cdot \nabla)\boldsymbol{E_0}$$

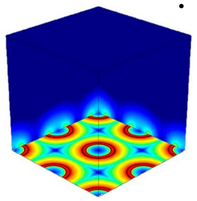

- DEP chip technology from Biological Dynamics (San Diego, CA) enables collection of biomarkers, at the circumferences of planar electrodes (red), directly from undiluted small volumes (30 µL) of blood plasma.[4]
- Ibsen *et al.* demonstrated immunofluorescent labeling of CD63 on the surfaces of glioblastoma exosomes isolated via DEP from undiluted human plasma.[5]

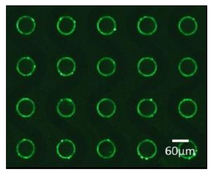

ALGORITHM OUTPUT CHARACTERISTICS

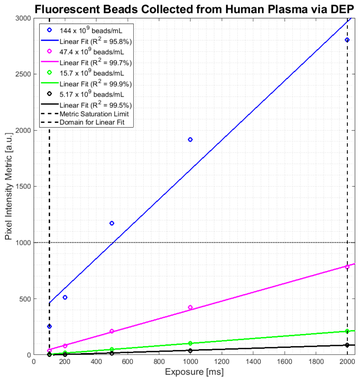

Fig. 1: Fluorescent nanoparticles (d = 100 nm) were spiked into healthy blood plasma and collected via DEP. Images of one field-of-view were taken at five exposures (100, 200, 500, 1000, 2000 ms) for four nanoparticle concentrations (contours at left). Data were fitted using all exposure values. Algorithm output (pixel intensity metric) were linear with respect to exposure for values between approx. 1 and 1000 a.u. The quality of fit decreased as values exceeded 1000 a.u., indicating saturation in output. Linearity over unsaturated output was anticipated because the signal-to-noise ratio remained constant with respect to exposure. The signal-to-noise ratio apparently decreased as exposure increased for saturated output.

Fig. 2: Images of four nanoparticle concentrations (contours at right) were taken at five exposures (100, 200, 500, 1000, 2000 ms). Data were fitted as second-degree polynomials across the three lowest concentrations. Predictions exceeded output (> 1000 a.u.) for the highest concentration of beads at 500, 1000, and 2000 ms exposures. Predictions were consistent with output (< 1000 a.u.) at the highest concentration of beads for 100 and 200 ms exposures. Output values above 1000 a.u. appeared to saturate. Values between approx. 1 and 1000 a.u. exhibited quadratic behavior with respect to concentration because the signal-to-noise ratio increased as concentration increased.

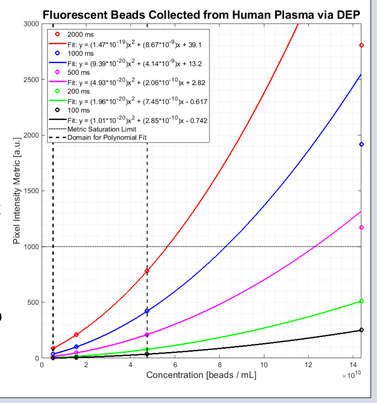

QUANTIFICATION & NORMALIZATION OF IMMUNOFLUORESCENTLY LABELED EXTRACELLULAR VESICLES

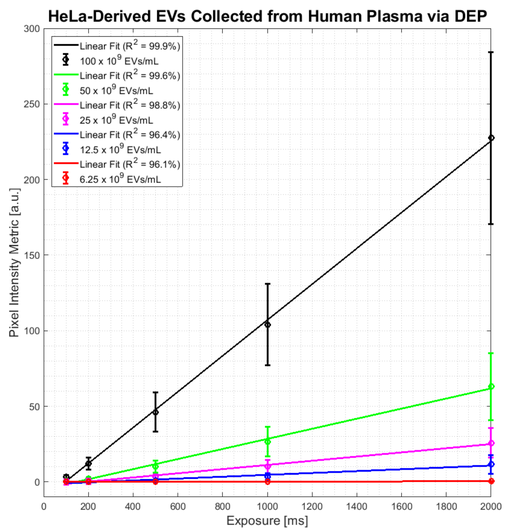

Fig. 3: Extracellular vesicles (EVs) were harvested from purified HeLa cell culture media and immuno-labeled with anti-CD9-AF555 primary antibody. Labeled EVs were spiked into healthy blood plasma and collected via DEP. Images of one field-of-view were taken at five exposures (100, 200, 500, 1000, 2000 ms) for four nanoparticle concentrations (contours at left). Data were fitted using all five exposure values. As anticipated from studies with fluorescent nanoparticles, algorithm output (pixel intensity metric) behaved linearly with respect to exposure for all values (< 1000 a.u.). The quality of fit decreased as concentration decreased, suggesting output values under approx. 1 a.u. were below the limit of detection. Combined with Fig. 1, this figure established a dynamic range of approx. 1 to 1000 a.u. for the algorithm. Each datum showed an average value across three replicates (n = 3) with error bars indicating standard deviations.

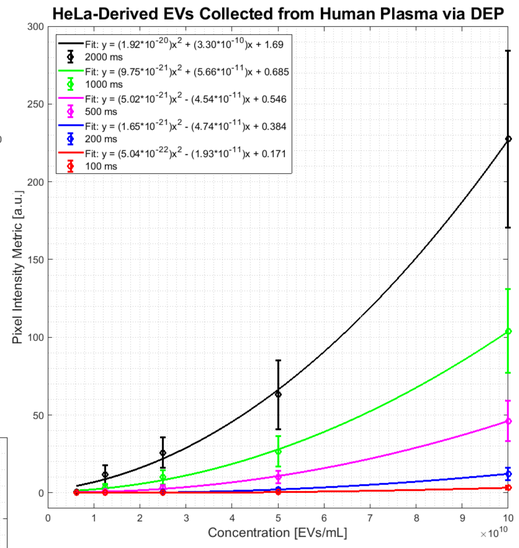

Fig. 4: Images of five EV concentrations (contours at right) were taken at five exposures (100, 200, 500, 1000, 2000 ms). Data were fitted as second-degree polynomials across all concentrations because output values remained below the saturation limit (1000 a.u.). Each datum shows an average value across three replicates (n = 3) with error bars indicating standard deviations.

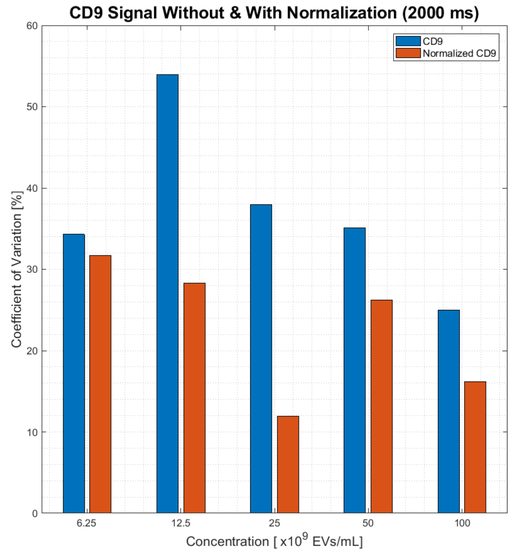

Fig. 5: Fluorescent nanoparticles ("internal standard") were introduced to five samples of EVs spiked into healthy blood plasma. Each sample contained a unique concentration of EVs and a constant concentration of nanoparticles. Induction of DEP enabled simultaneous collection EVs and nanoparticles. Differences in nanoparticle fluorescence indicated differences in collection efficiency of DEP chips. Normalizing EV fluorescence to respective nanoparticle fluorescence controlled for chip-to-chip variation. The figure at left showed reductions in the coefficient of variation (CV ≡ standard deviation / mean) of EV fluorescence (signal from immunolabeled CD9) compared to the CV of normalized EV fluorescence (CD9 signal / nanoparticle signal) at all five concentration values for images taken at 2000 ms exposure. The internal standard did not completely eliminate variability in replicates likely due to other sources of error (e.g. pipetting).

FLUORESCENCE QUANTIFICATION ALGORITHM

1. A mapping of electrode locations is extracted from the bright field image and projected onto the corresponding fluorescence image. Fixed square areas of pixels, centered at each electrode, are extracted from fluorescence images for analysis.

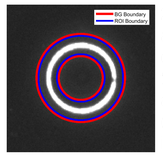

2. Fixed boundaries are applied across each electrode area to categorize pixels as background (**BG**) or region-of-interest (**ROI**).

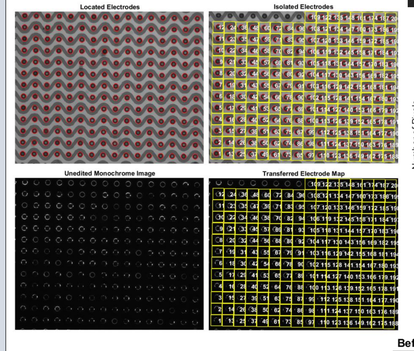

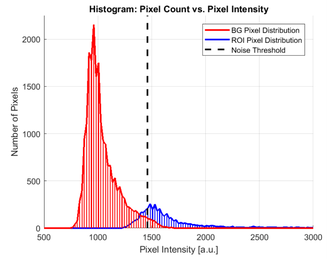

3. Statistical analysis of BG pixels establish a **noise threshold** for each electrode area.

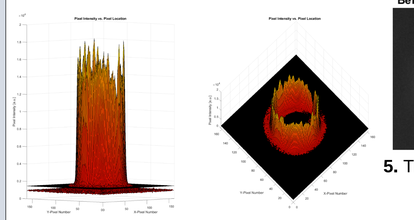

5. The noise threshold for a given electrode area is subtracted from each pixel.

4. The black horizontal plane corresponds to the dotted black line (noise threshold) in **3**.

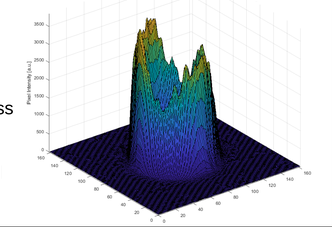

6. Pixel intensities at respective locations across all electrode areas are averaged, yielding the above image. Pixel intensities in the resultant image are then averaged to generate the **pixel intensity metric**.

CONCLUSIONS

- Automated quantification of fluorescently labeled surface proteins on EVs collected via DEP eliminates user bias in analysis of isolated biomarker concentrations.
- Algorithm output scales linearly with exposure and quadratically with concentration over a dynamic range of approx. four orders of magnitude (1 to 1000 a.u.).
- Normalization of biomarker signal to an internal standard (i.e. fluorescent nanoparticles spiked into the sample) reduces the coefficient of variation by controlling for differences in collection efficiency across DEP chips.

FUTURE DIRECTIONS

- Optimize and standardize procedures that affect image quality (e.g. sample preparation, DEP collection, washing, staining, microscope settings) across users.
- Implement a fluorescent membrane dye as a new internal standard to:
  1. maximize EV collection by eliminating collection of fluorescent nanoparticles;
  2. generate a metric for surface protein expression on collected EVs
- Utilize the algorithm for multivariate analysis of clinical datasets of immunolabeled cancer biomarkers collected via DEP from undiluted blood plasma.

References: 1. Pohl, H.A., *et al. J Biol Phys* (1978); 2. Pohl, H.A. *J Appl Phys* (1951); 3. Pethig, R. "Dielectrophoresis" (2017); 4. Heineck, D. (PhD Thesis; UCSD, 2016); 5. Ibsen, S.D. *et al. ACS Nano* (2017).
Acknowledgements: K.T.G. would like to acknowledge the Achievement Rewards for College Scientists (ARCS) Foundation Oregon for their financial support.